Medical Oncology (2025) 42:257
https://doi.org/10.1007/s12032-025-02801-6

ORIGINAL PAPER

Tumor-derived CXCL5 promotes 5-fluorouracil resistance in colorectal cancer cells via p21 downregulation

Wanjun Xu[1] · Jianjun Wang[3] · Wencan Han[1] · Jinmin Sun[1] · Xuemei Yang[1] · Xiaomin Li[1,2] · Dongsheng Pei[1]

Received: 14 March 2025 / Accepted: 16 May 2025

Abstract

The efficacy of 5-fluorouracil treatment for colorectal cancer (CRC) is substantially compromised by drug resistance, although the underlying mechanisms remain unclear. In this research, we aimed to explore the role and mechanism of action of CXC motif chemokine ligand 5 (CXCL5) in 5-fluorouracil resistance. RNA sequencing was conducted to detect abnormally expressed genes in the 5-fluorouracil-resistant colon cancer cell line, HCT8-5FU. CXCL5 expression in CRC tissues and cell lines was evaluated using RT-qPCR, western blotting, and immunohistochemistry. In vivo and in vitro assays were conducted to evaluate the role of CXCL5 in the promotion of CRC progression. Mass spectrometry and co-immunoprecipitation were employed to investigate the role of CXCL5 in CRC development and 5-fluorouracil resistance. Immunofluorescence and western blot analyses were employed to determine the subcellular localization of CXCL5 and its associated signaling pathways. CXCL5 expression was elevated in both CRC tissues and cell lines. CXCL5 promoted CRC cell growth and resistance to 5-fluorouracil in both in vitro and in vivo settings. Mechanistically, CXCL5 may modulate the MDM2/p53 axis to inhibit p21 by binding to RALY. In this study, CXCL5 accelerated CRC progression and increased CRC cell resistance to 5-fluorouracil via the inhibition of p21 expression. Thus, CXCL5 is a potential target for CRC therapeutic strategies.

Keywords Colorectal cancer · CXCL5 · 5-fluorouracil · p21

Abbreviations

CRC	Colorectal cancer
Co-IP	Coimmunoprecipitation
CXCL5	C-X-C motif chemokine ligand 5
siRNA	Small interfering RNA
CCK-8	Cell™ Counting Kit-8
shRNA	Short hairpin RNA
IHC	Immunohistochemistry
IF	Immunofluorescence
MS	Mass spectrometry
RT-qPCR	Real-time quantitative polymerase chain reaction
5-FU	5-Fluorouracil

Introduction

As the second most common malignant solid tumor worldwide, colorectal cancer (CRC) is also responsible for the third highest tumor-related death rate in the world [1, 2]. Therefore, further research on this disease is required. Surgery combined with chemoradiotherapy remains the first-line treatment for CRC [3]. 5-Fluorouracil (5-FU) is one of the drugs of choice for chemotherapy. However, drug resistance limits its therapeutic benefits. To improve the prognosis of patients with CRC, the molecular mechanisms underlying chemotherapy resistance during CRC development must be investigated.

Chemokines are small signaling proteins that help immune cells migrate to damaged tissues or diseased organs,

Wanjun Xu, Jianjun Wang and Wencan Han share first authorship.

✉ Xiaomin Li
lxm1980326@sina.com

✉ Dongsheng Pei
dspei@xzhmu.edu.cn

[1] Department of Pathology, Laboratory of Clinical and Experimental Pathology, National Demonstration Center for Experimental Basic Medical Science Education, School of Basic Medical Sciences, Xuzhou Medical University, Xuzhou 221004, Jiangsu, China

[2] Department of Gastroenterology, Clinical Medical Research Center, Suqian Clinical College, Xuzhou Medical University, Suqian 223800, Jiangsu, China

[3] Department of Histology and Embryology, Wannan Medical College, Wuhu 241002, Anhui, China

Published online: 13 June 2025

especially in the presence of inflammation. Chemokines are categorized into four conserved groups (C, CC, CXC, and CX3C) based on the NH2-terminal cysteine residues. Chemokines and their receptors regulate the transcription of various genes. This facilitates various cellular physiological activities such as growth, development, differentiation, and apoptosis [4]. Recent evidence increasingly suggests that chemokines are crucial for tumor development. Chemokines produced by tumor and stromal cells contribute to the recruitment of tumor-associated white blood cells, promote angiogenesis, facilitate malignant cell proliferation and metastasis, and induce fibroblast activation. Chemokines and their receptors play crucial roles in the inflammatory microenvironment, which has been identified as the seventh hallmark of cancer. The dysregulation of chemokines has been observed in numerous tumors, and certain chemokines are associated with unfavorable prognoses in patients with cancer [5–10].

CXC motif chemokine ligand 5 (CXCL5), also referred to as epithelial-derived neutrophil-activating peptide 78 (ENA-78), was initially identified as a strong chemokine and activator of neutrophil function [11]. When bound to its receptor, CXC motif chemokine receptor 2 (CXCR2), CXCL5 is involved in various biological activities, including the promotion of angiogenesis, remodeling of connective tissue, and neutrophil chemotaxis [12–14]. Increasing evidence suggests that CXCL5 plays a role in cancer-related inflammation and various malignant processes in cancer biology. In addition, CXCL5 is abnormally expressed in various tumors. Elevated CXCL5 expression has been noted in gastric, prostate, squamous cell, hepatocellular, and pancreatic cancers and correlates with tumor stage, local invasion, neutrophil infiltration, and metastatic potential [15–19]. Recent research suggests that CXCL5 may serve as a prognostic biomarker of cancer [20]. However, most studies to date have been small and yielded inconsistent results, leaving its prognostic value uncertain.

In previous studies, high-throughput sequencing has been used to identify elevated CXCL5 expression in 5-FU-resistant colon cancer cell lines. However, the association between CXCL5 and 5-FU resistance in CRC has not been reported. Therefore, in this study, we aimed to explore the role and mechanism of action of CXCL5 in 5-FU resistance.

Methods

Cell culture

Human CRC cell line HCT8 and its 5-FU-resistant cell line HCT8-5FU were obtained from the Chinese Tissue Culture Collections (MeisenCTCC, Hangzhou, China). Human colorectal cancer cell lines (HT29, SW480, SW620, HCT-116, Ls174t) and normal colon mucosal epithelial cell line (FHC) were sourced from the American Type Culture Collection (ATCC, Manassas, VA, USA). HCT8-5FU cells were maintained at 37 °C in a 5% CO_2 humidified atmosphere using RPMI 1640 medium supplemented with 10% fetal bovine serum and 0.5 μg/ml 5-FU (H31020593, Shanghai Xudong Haipu Pharmaceutical Co., Ltd., China). The other cells were all cultured in RPMI 1640 medium supplemented with 10% fetal bovine serum (3032A, Umedium, Hefei, China) at 37 °C under 5% CO_2 in a humidified environment.

RNA extraction, library construction, BioProject accession and bioinformatics analysis of RNA-seq

RNA extraction

Total RNA was isolated and purified using TRIzol reagent (Invitrogen, Carlsbad, CA, USA) following the manufacturer's procedure. The RNA amount and purity of each sample were quantified using NanoDrop ND-1000 (NanoDrop, Wilmington, DE, USA). The RNA integrity was assessed by Bioanalyzer 2100 (Agilent, CA, USA) with RIN number > 7.0, and confirmed by electrophoresis with denaturing agarose gel. Approximately 2 μg of total RNA was used to remove ribosomal RNA according to the manuscript of the Epicentre Ribo-Zero Gold Kit (Illumina, San Diego, USA).

Library construction

Following purification, the ribo-minus RNA was fragmented into small pieces using Magnesium RNA Fragmentation Module (NEB, cat.e6150, USA) under 94 °C 5–7 min. Then the cleaved RNA fragments were reverse-transcribed to create the cDNA by SuperScript™ II Reverse Transcriptase (Invitrogen, cat. 1896649, USA), which were next used to synthesise U-labeled second-stranded DNAs with E. coli DNA polymerase I (NEB, cat.m0209, USA), RNase H (NEB, cat.m0297, USA) and dUTP Solution (Thermo Fisher, cat.R0133, USA). An A-base was then added to the blunt ends of each strand, preparing them for ligation to the indexed adapters. Each adapter contains a T-base overhang for ligating the adapter to the A-tailed fragmented DNA. Single- or dual-index adapters are ligated to the fragments, and size selection was performed with AMPureXP beads. After the heat-labile UDG enzyme (NEB, cat.m0280, USA) treatment of the U-labeled second-stranded DNAs, the ligated products are amplified with PCR by the following conditions: initial denaturation at 95 °C for 3 min; 8 cycles of denaturation at 98 °C for 15 s, annealing at 60 °C for 15 s, and extension at 72 °C for 30 s; and then final extension at 72 °C for 5 min. The average insert size for the final cDNA

library was 300 ± 50 bp. At last, we performed the 2 × 150 bp paired-end sequencing (PE150) on an illumina Novaseq™ 6000 (LC-Bio Technology CO., Ltd., Hangzhou, China) following the vendor's recommended protocol.

BioProject accession

The raw RNA-seq data have been submitted to the NCBI Sequence Read Archive (SRA) database: 1. https://www.ncbi.nlm.nih.gov/sra/PRJNA1189255; 2. https://www.ncbi.nlm.nih.gov/sra/PRJNA1190160.

Bioinformatics analysis of RNA-seq

Fastp was used to remove the reads that contained adaptor contamination, low quality bases and undetermined bases. Then sequence quality was also verified using fastp. We used Bowtie2 and Tophat2 to map reads to the genome of *Homo sapiens* GRCh38. The mapped reads of each sample were assembled using StringTie. Then, all transcriptome from all samples were merged to reconstruct a comprehensive transcriptome using gffcompare (https://github.com/gpertea/gffcompare/). After the final transcriptome was generated, StringTie was used to estimate the expression levels of all transcripts. Transcripts were annotated with known mRNAs, known long non-coding RNAs (lncRNAs) and transcripts shorter than 200 nt were discarded. Then we utilized CPC and CNCI to predict transcripts with coding potential. All transcripts with CPC score < − 1 and CNCI score < 0 were removed. The remaining transcripts with class code (I, j, o, u, x) were considered as lncRNAs. StringTie was used to perform expression level for mRNAs and lncRNAs by calculating FPKM {FPKM = [total_exon_fragments/mapped_reads(millions) × exon_length(kB)]}. The differentially expressed mRNAs and lncRNAs were selected with log2 (fold change) > 1 or log2 (fold change) < − 1 and with parametric F-test comparing nested linear models (*P* value < 0.05) by R package edgeR.

CRC tissues

Thirty-five pairs of colorectal cancer (CRC) and adjacent noncancerous tissues were collected from The Affiliated Hospital of Xuzhou Medical University in Xuzhou, China. We extracted RNA from 26 pairs of colorectal carcinoma and para-carcinoma tissues. The study was approved by the Ethics Committee of Xuzhou Medical University, and all patients gave their consent for the use of clinical materials in research. CRC tissues were obtained from surgically resected specimens, while adjacent non-cancerous tissues were collected near the tumor margins. Specimens were rapidly frozen in liquid nitrogen until needed. Pathologists diagnosed all samples as adenocarcinoma.

Construction and transfection of small interfering RNA (siRNA), lentivirus, and vectors

All siRNAs were designed and synthesized by GenePharma (Suzhou, China) (Table S1). GenePharma also constructed and packaged sh-CXCL5 lentivirus vectors into lentivirus particles. Ruibiotech constructed all the vectors utilized in the study (Guangzhou, China). siRNAs or vectors were used to transfect CRC cells with using the Lipo8000™ Transfection Reagent (C0533-1.5 ml, Beyotime, China) following the manufacturer's protocol.

RNA extraction, reverse transcription, polymerase chain reaction (PCR), and real-time quantitative PCR (RT-qPCR)

Total RNA extraction was performed with RNAiso Plus (9108, TaKaRa, Japan) as per the manufacturer's instructions. Total RNA was quantified using a Nanophotometer (Implen, Germany) and reverse-transcribed into cDNA with PrimeScript™ RT Master Mix (Perfect Real Time) (RR036A, TaKaRa, Japan). cDNA detection was performed using a mixture of 1μL cDNA, 0.8μL gene-specific primers, 9.2 μL nuclease-free water, and 10μL SYBR Green qPCR Master Mix (G3322-05, Servicebio, Wuhan, China) on an Applied Biosystems instrument (Thermo Fisher Scientific, USA). Relative mRNA quantification was performed by the ΔΔCt method and GAPDH was the internal reference used in the RT-qPCR procedure. All primers utilized in the study were synthesized by Sangon Biotech, Shanghai, China (Table S2).

CCK-8

To assess CXCL5's impact on cell proliferation, 2×10^3 cells were seeded into each well of 96-well plates. Cell proliferation was assessed using the Cell Counting Kit-8 (CCK-8) (E1CK-000208, EnoGene, China) by measuring the absorbance at 450 nm at specified time intervals.

Colony formation

After seeding cells at a density of 1×10^3 per well in 6-well plates, they were treated with 5-FU (0.5 μg/ml) for 14 days. The cell culture medium with or without 5-FU was changed

every three days. Colonies were treated with 4% paraformaldehyde (PFA) (G1101, Servicebio, Wuhan, China) and stained using 0.1% crystal violet (VS1003, VICMED, China) to evaluate growth. Finally, the cell colonies were imaged and counted.

EdU cell proliferation detection

Cell proliferation was assessed using the BeyoClick™ EdU Cell Proliferation Kit with Alexa Fluor 594 (C0078S, Beyotime China) following the manufacturer's guidelines. Briefly, cells were incubated with a 1 × EdU working solution for 2 h. Subsequently, the cells underwent fixation, washing, and incubation with the reaction solution at room temperature as per the provided instructions. The nucleus was stained using DAPI (KGA512, KeyGen Biotech, China). The positive cell count was determined and computed.

Flow cytometry

Cells were harvested following treatment with 5-FU.Cells were exposed to 70% ethanol and stored overnight at 4 °C. Sample cells were incubated using the Cell Cycle Detection Kit (KGA512, KeyGen Biotech, China) following the provided instructions. Cell cycle progression was analyzed using a BD FACSVerse flow cytometer (Becton, Dickinson and Company, USA).

Subcutaneous tumor model

All animal experimental protocols were approved by the Animal Care and Use Committee of Xuzhou Medical University. Male BALB/C nude mice, aged three to four weeks, were obtained from GemPharmatech Co., Ltd.

ELISA

Cell culture supernatants were obtained, and the human CXCL5 content was evaluated using the Human ENA-78/CXCL5 ELISA kit (JM-04667H1, JINGMEI, China) according to the instruction and the value of absorption was assessed at 450 nm.

In vitro and in vivo treatment with 5-FU

SW620 and HCT-8 cells were exposed to 0.5 μg/ml 5-FU, while HCT8-5FU cells received either 3 μg/ml or 0.5 μg/ml 5-FU for 24 h, for subsequent CCK8, EdU, and colony formation assays. We also created subcutaneous tumor models using HCT8-5FU cells with either stable CXCL5 knockdown or control cells in the vivo experiment. Nude mice with subcutaneous tumors measuring 0.5 cm were administered 20 μg of 5-FU per gram of body weight via intraperitoneal injection, whereas the control group received saline, three times per week.

Immunofluorescence (IF)

To confirm the expression and localization of CXCL5 in HCT8-5FU, IF was performed in confocal dishes. In the IF assays, the antibody (1:200, R389303, Zenbio, China) and DyLight 594-labeled goat anti-rabbit IgG (1:1000, RS23420, ImmunoWay, USA) were utilized. Images were obtained under a confocal microscope. Fluorescent images were captured using a laser scanning confocal microscope (Leica STELLARIS 5, Germany).

Mass spectrometry (MS) and Co-immunoprecipitation (Co-IP)

Proteins interacting with CXCL5 were isolated and subjected to SDS-PAGE, then visualized using the Fast Silver Stain Kit (#P00175, Beyotime, Shanghai, China). The distinct protein band was then cut out and identified using MS. The Co-IP assays utilized rabbit control IgG (30000–0-AP) from Proteintech (USA). The enrichment of RALY was confirmed using Western blot analysis (1:2000, BD-PT3997, Biodragon, China).

Western blot

One-Step PAGE Gel Fast Preparation Kit (PG212, PG214, Shanghai, China) was used to prepare gel. Total protein was separated by SDS-PAGE and transferred onto PVDF membranes. The membranes were blocked for 10 min using a fast-blocking buffer (P30500, NCM Biotech, Suzhou, China). Subsequently, the PVDF membranes were incubated overnight at 4 °C with the following primary antibodies: anti-CXCL5 (1:1000, R389303, Zenbio, China), anti-p21 (1:1000, 381102, Zenbio, China), anti-GAPDH (1:2000, 10094–1-AP, Proteintech, USA), anti-RALY (1:2000, BD-PT3997, Biodragon, China), anti-MDM2 (1:2000, BD-PT2692, Biodragon, China), and anti-P53 (1:2000, 60283–2-lg, Proteintech, USA).The next day, membranes were incubated with Peroxidase Conjugated secondary antibodies (1:10000, FDR007 or FDM007, FDbio, China) for two hours at room temperature. The protein bands were observed using FDBio-Dura ECL Kit (FD8020, FDbio,

China). All antibodies were diluted with antibody diluent (WB500D, NCM Biotech, Suzhou, China).

Immunohistochemistry (IHC)

Samples were submitted to Biossic Biotechnologies Company Limited in Hubei, China, for immunohistochemistry (IHC) staining. H-Score calculations were conducted to assess IHC staining in our study. The assay utilized anti-CXCL5 primary antibodies (1:100, 252002, Zenbio, China).

Separation of cytoplasm and nucleus fraction

Separation of cytoplasm and nucleus fraction was performed using the Minute nuclear plasma separation kit (#SC-003, Invent Biotechnologies, USA) according to the instruction. Then, the extracts were suffered from Western blotting detection. GAPDH was used as cytoplasmic internal reference and H3 was used as nuclear internal reference.

Statistical analyses

GraphPad Prism 8.0 (GraphPad Software, La Jolla, CA, USA) was used for statistical analysis. Data are expressed as mean ± standard deviation. A two-sample Student's T-test was employed to compare the two groups. Using the paired t-test, the study analyzed CXCL5 expression in CRC tissues versus matched noncancerous tissues. Significance levels were set at $*P<0.05$, $**P<0.01$, $***P<0.001$, and $****P<0.0001$. NS: not significant.

Results

CXCL5 is elevated in 5-FU-resistant colon cancer cell line HCT8-5FU

We confirmed the drug resistance of HCT8-5FU using the Cell Counting Kit (CCK)-8 assay. Compared with the 5-FU-sensitive HCT-8 cell line, the half-maximal inhibitory concentration of 5-FU was significantly upregulated in HCT8-5FU cells (Fig. 1A). To investigate the 5-FU resistance mechanism of HCT8-5FU cells, we conducted RNA sequencing of HCT8-5FU and HCT8 cells. This identified several differentially expressed genes in HCT8-5FU cells, among which *CXCL5* was the most upregulated gene (Fig. 1B–D). RT-qPCR confirmed the upregulation of *CXCL5* expression in HCT8-5FU cells (Fig. 1E). Western blotting and immunofluorescence assays further demonstrated that the CXCL5 protein was highly expressed in HCT8-5FU cells (Fig. 1F–H). Taken together, we confirmed the high expression of CXCL5 in HCT8-5FUcells.

CXCL5 is upregulated in CRC tissues and cell lines

We investigated the expression levels of CXCL5 in CRC tissues and cells. Using the Gene Expression Profiling Interactive Analysis database, we discovered that CXCL5 was upregulated in CRC (colon and rectum adenocarcinoma) tissues (Fig. 2A). Our analysis of 26 pairs of CRC and adjacent tissues also revealed the upregulation of CXCL5 in CRC tissues (Fig. 2B). Immunohistochemical assays confirmed the high level of CXCL5 expression in CRC tissues (Fig. 2C). Subsequently we used RT-qPCR and western blotting to compare CXCL5 expression in normal colonic mucosal epithelial cells (FHC) with that in six CRC cell lines. The expression level of CXCL5 was elevated in CRC cells (Fig. 2D–F). These findings suggest that CXCL5 is significantly overexpressed in CRC tissues and cells.

Knockdown of CXCL5 enhances the sensitivity of CRC cells to 5-FU

To investigate the role of CXCL5 in CRC, the gene in HCT8-5FU and HCT8 cells was downregulated via siRNAs or shRNAs (Fig. 3A and B). Given that 5-FU induces apoptosis and suppresses tumor cell proliferation, we investigated whether CXCL5 contributes to cancer progression by enhancing tumor cell proliferation or reducing apoptosis. We first investigated the effect of CXCL5 knockdown on apoptosis; however, no significant effect was observed. Subsequently, we focused on whether CXCL5 promoted cell proliferation. A CCK-8 assay revealed that downregulation of CXCL5 enhanced the growth inhibition of HCT8-5FU and HCT8 cells by 5-FU (Fig. 3C and D). 5-Ethynyl-2′-deoxyuridine (EdU) assays indicated that CXCL5 knockdown suppressed the proliferation of HCT8-5FU and HCT8 cells upon 5-FU treatment (Fig. 3E, F, and I). Through colony formation assays, we also discovered that downregulation of CXCL5 inhibited the clonogenesis of HCT8-5FU and HCT8 cells (Fig. 3G, H, and J).

For vivo experiments, we constructed subcutaneous tumor models in nude mice. In alignment with the in vitro functional experiments, these indicated that CXCL5 knockdown in HCT8-5FU cells increased their sensitivity to 5-FU in vivo (Fig. 3K, L and S1). Thus, both in vitro and in vivo experiments revealed that CXCL5 knockdown increased the sensitivity of CRC cells to 5-FU.

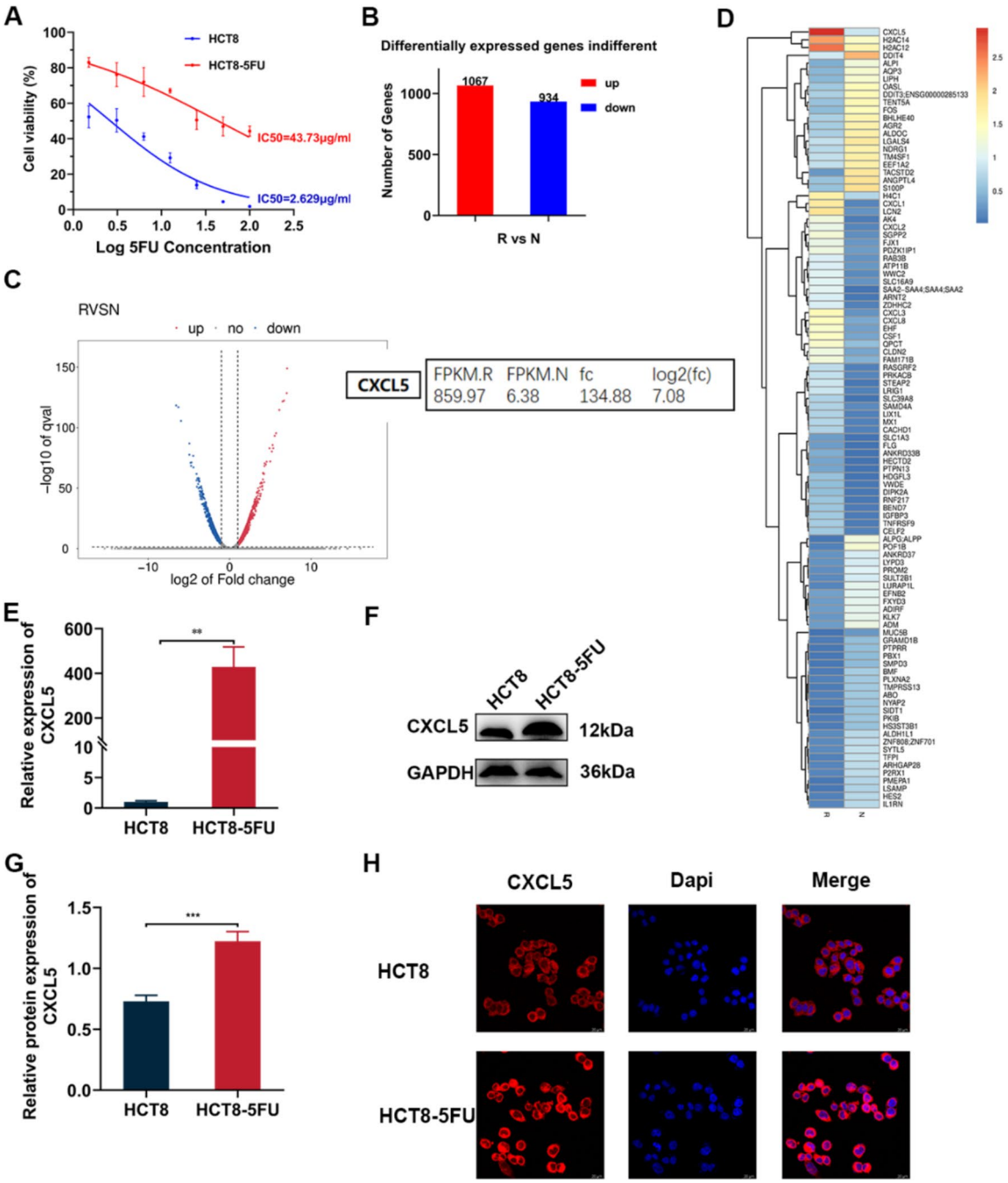

Fig. 1 CXCL5 is elevated in CRC 5-FU resistant cell line HCT8-5FU. **A** CCK-8 assays identified the 5-FU IC50 of HCT8-5FU cells. **B** RNA-seq identified differentially expressed genes in the 5-FU-resistant cell line HCT8-5FU. **C** and **D** Volcano plot and heat map displaying that the expression of *CXCL5* was the highest among the differentially expressed genes in HCT8-5FU cells. **E** RT-qPCR showed that the expression of *CXCL5* was higher in HCT8-5FU cells than that in HCT8 cells. $^{**}P < 0.01$. **F** and **G** Western blotting demonstrated that CXCL5 was more highly expressed in HCT8-5FU cells than that in HCT8 cells. $^{***}P < 0.001$. **H** Immunofluorescence assays showed that CXCL5 expression was higher in HCT8-5FU cells than that in HCT8. Scale bar: 20 μm

Overexpression of CXCL5 promotes resistance of CRC cells to 5-FU

To confirm the role of CXCL5 in CRC, we increased its expression in SW620 and HCT8 cells using an overexpression vector (Figs. 4A, B, S2A, and S2B). Similarly, CCK-8 and EdU assays were conducted to evaluate the impact of CXCL5 expression on cellular functions. The CCK-8 assays indicated that elevated CXCL5 levels decreased the sensitivity of CRC cells to 5-FU (Fig. 4C

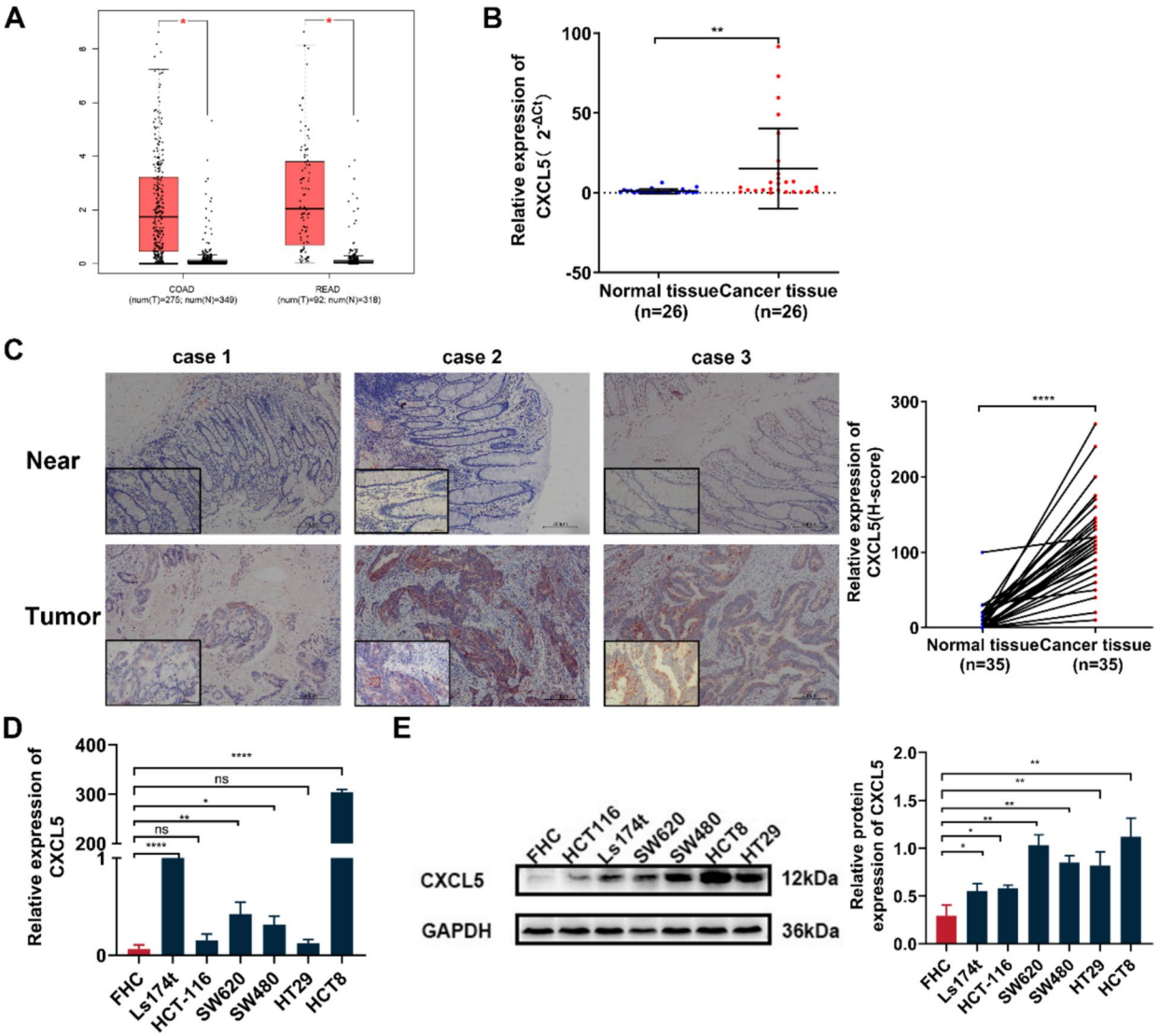

Fig. 2 CXCL5 is upregulated in CRC tissues and cell lines. **A** In the GEPIA database, *CXCL5* was upregulated in COAD and READ. **B** RT-qPCR revealed that the expression levels of *CXCL5* were higher in the cancer tissues of 26 patients with colon cancer than those in the matched adjacent tissues. $^{**}P<0.01$. **C** Representative immunohistochemistry images show that CXCL5 was more highly expressed in CRC tissues than in the adjacent tissues. Scale bar: 200 μm. $^{****}P<0.0001$. **D** RT-qPCR displayed a higher expression level of CXCL5 in CRC cells than that in normal colonic mucosal epithelial cells. $^{*}P<0.05$, $^{**}P<0.01$, $^{***}P<0.001$, $^{****}P<0.0001$, *NS* not significant. **E** and **F** Western blot assays indicated that the CXCL5 protein was overexpressed in CRC cells compared with that in normal colonic mucosal epithelial cells. $^{*}P<0.05$, $^{**}P<0.01$

and D). The EdU assays indicated that overexpression of CXCL5 promoted the proliferation of SW620 and HCT8 cells treated with 5-FU (Fig. 4E–G). Colony formation assays revealed that CXCL5 overexpression improved the colony formation ability of SW620 and HCT8 cells treated with 5-FU (Fig. 4H–J). These assays demonstrated that CXCL5 overexpression promotes 5-FU resistance in CRC cells.

Expression of cell cycle suppressor gene CDKN1A (p21) is downregulated by CXCL5

Upon RNA sequencing and Kyoto Encyclopedia of Genes and Genomes (KEGG) analysis of HCT8-5FU cells, we noticed the enrichment of differentially expressed genes in cell cycle pathways (Fig. 5A). Upon downregulation of CXCL5 in HCT8-5FU cells and RNA sequencing, we

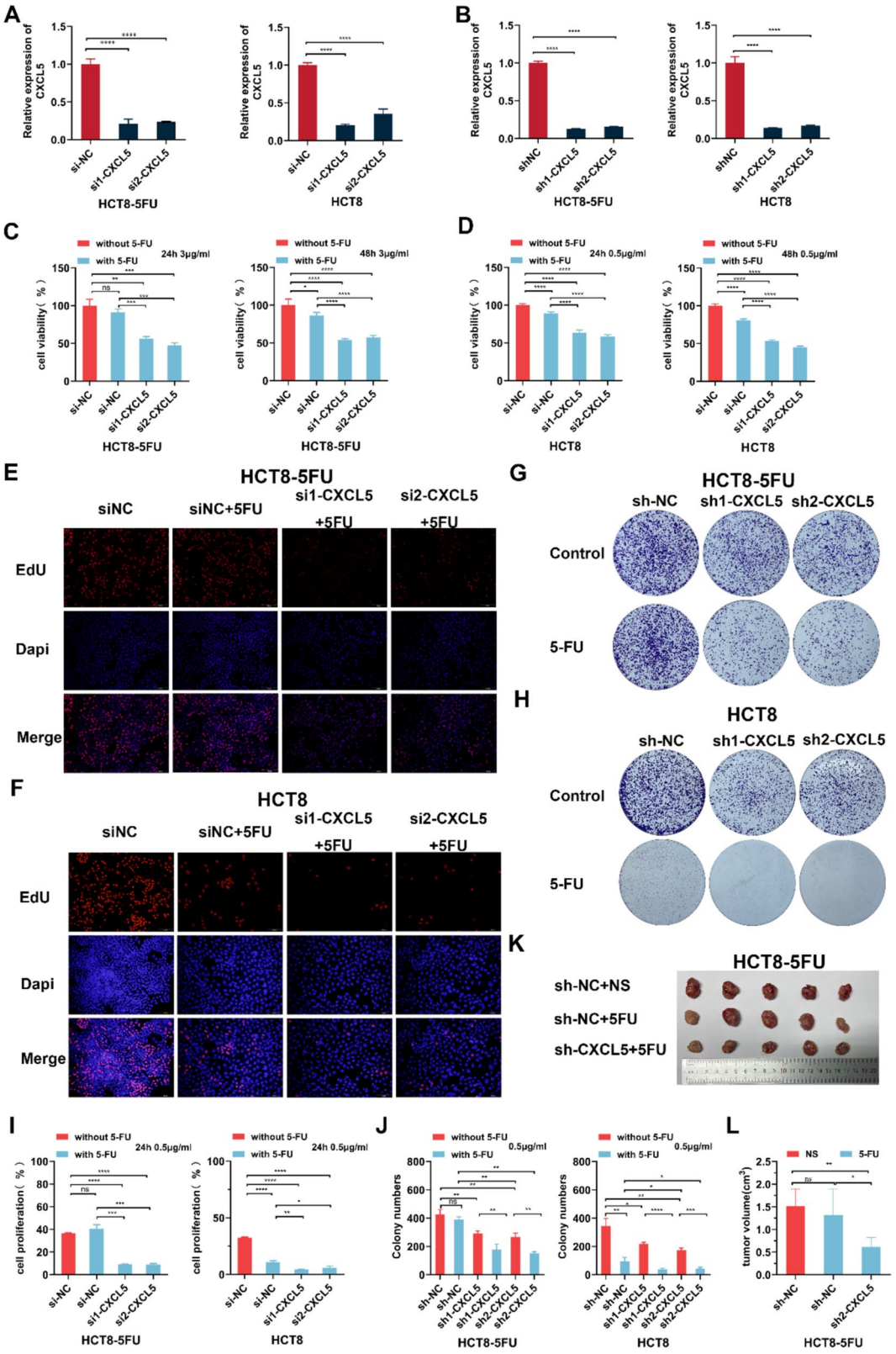

also discovered the enrichment of differentially expressed genes in cell cycle pathways. Flow cytometry assays were used to explore whether CXCL5 promotes the cell cycle of CRC cells. We discovered that a decrease in the CXCL5 level enhanced the cell cycle arrest of CRC cells, whereas an increase in the CXCL5 level accelerated the cell cycle

◂**Fig. 3** Knockdown of *CXCL5* enhances the sensitivity of CRC cells to 5-FU. **A** and **B** RT-qPCR assays revealed the expression of *CXCL5* in HCT8-5FU and HCT8 cells after transfection with siRNAs or lentiviruses. ****$P < 0.0001$. **C** and **D** CCK-8 assays indicated that lower CXCL5 levels suppressed the 5-FU resistance of CRC cells. *$P < 0.05$, **$P < 0.01$, ***$P < 0.001$, ****$P < 0.0001$. *NS* not significant. **E** and **F** EdU assays revealed that *CXCL5* knockdown suppressed the 5-FU resistance of CRC cells. Scale bar: 200 μm. *$P < 0.05$, **$P < 0.01$, ***$P < 0.001$, ****$P < 0.0001$, *NS* not significant. **G—J** Colony formation assay demonstrated that knockdown of CXCL5 expression inhibited clone formation ability of HCT8-5FU and HCT8. *$P < 0.05$, **$P < 0.01$, ***$P < 0.001$, ****$P < 0.0001$, *NS* not significant. **K** and **L** subcutaneous tumors with stable *CXCL5* silencing had higher 5-FU sensitivity than control cells. *$P < 0.05$, **$P < 0.01$, *NS* not significant

of CRC cells (Figure S3A–D). We analyzed the intersection between the two sets of enriched genes in the cell cycle pathways, revealing three genes: CDC25A, CDKN1A, and CDKN1C (Fig. 5B and C). The abovementioned cell cycle-related genes were verified and screened using RT-qPCR assays, and changes in CDKN1A expression attracted our attention. CDKN1A (p21) was downregulated in HCT8-5FU cells, whereas its expression was restored after CXCL5 was downregulated (Fig. 5D and E). We also discovered that CDKN1A expression was downregulated following CXCL5 overexpression in HCT8 and SW620 cells (Fig. 5F and G). We observed the same results in western blot assays: protein levels of p21 were downregulated in HCT8-5FU cells (Fig. 5H and S3E). Lower levels of CXCL5 resulted in upregulation of p21 expression, whereas higher levels of CXCL5 had the opposite effect (Fig. 5I, J, S3F and S3G). CCK-8 assay demonstrated that overexpression of CDKN1A (p21) had an inhibitory effect on the proliferation capacity of HCT8-5FU cells with high expression of CXCL5 (Figure S3H).

CXCL5 modulates MDM2/p53 axis to inhibit p21 by binding to RALY

Given that CXCL5 was previously revealed as a secretory protein, we hypothesized that its extracellular secretion would suppress p21. We used an enzyme-linked immunosorbent assay kit to detect the secretion of CXCL5, which revealed no difference in CXCL5 secretion between HCT8 and HCT8-5FU cells (Fig. 6A). Hence, we investigated whether CXCL5 plays an intracellular inhibitory role on p21. To explore the mechanism by which CXCL5 suppresses p21, we attempted to identify the protein to which CXCL5 binds by using a co-immunoprecipitation (Co-IP) assay. After Co-IP, SDS-PAGE of IgG and anti-CXCL5 groups at the same position were selected, followed by a silver staining assay. Subsequently, mass spectrometry (MS) was performed for identification. Based on the MS results, we analyzed and screened the binding proteins identified as highly reliable in the two sets of data tables and excluded non-specific binding proteins (those that also bound to IgG; Fig. 6B). Ultimately, we identified four proteins of the expected size that bound specifically to CXCL5. Most of these were nuclear proteins. Immunofluorescence assays revealed that CXCL5 was expressed in the nuclei of HCT8-5FU cells (Fig. 6C). Western blot of cytoplasmic and nuclear fractions also confirmed that CXCL5 was expressed in the nucleus (Figure S4A). According to a previous study, RALY, one of the four predicted binding proteins, promotes tumor progression by increasing the stability of MDM2 and inhibiting p53 activity [21]. Upon KEGG network analysis, we discovered that p53 is upstream of p21. Therefore, we speculated that CXCL5 inhibits the p53 pathway by influencing RALY expression. The specific binding of CXCL5 to RALY was confirmed using a Co-IP assay (Fig. 6D and E). We compared RALY expression in HCT8 and HCT8-5FU cells and discovered that RALY was highly expressed in HCT8-5FU cells (Figs. 6F and S4B). Thus, overexpression of CXCL5 in HCT8 cells promoted the expression of RALY, which subsequently regulated the expression of MDM2 and inhibited the expression of p53 and p21. Downregulation of CXCL5 expression in HCT8-5FU cells resulted in the opposite changes in protein expression (Figs. 6G, H, S4C and S4D).

Discussion

Recent research on the role of chemokines in tumor progression has identified abnormal CXCL5 expression in various cancers. Our study demonstrates that CXCL5 is highly expressed in CRC. Our results align with those of previous studies in which CXCL5 was upregulated in various cancers, including glioblastoma; liver, non-small cell lung, breast, penile, melanoma, cervical, gastric, pancreatic, bladder, prostate, esophageal, nasopharyngeal, and thyroid cancer; clear cell carcinoma of the kidney; osteosarcoma; head and neck squamous cell carcinoma; bile duct carcinoma; and laryngeal squamous cell carcinoma [15, 16, 18, 19, 22–35]. Growing evidence has demonstrated that CXCL5 exerts cancer-promoting effects by mediating various cell behaviors during tumor development, including tumor proliferation, invasion and migration, angiogenesis, changes to the tumor microenvironment, and chemotherapy resistance. However, few reports on the correlation between CXCL5 expression and drug resistance in tumors have been published. In pancreatic cancer, elevated CXCL5 levels contribute to gemcitabine resistance by influencing both cancer and stromal cells [36]; Similarly, CXCL5 is upregulated in the mitomycin-C-resistant bladder cancer cell line M-RT4, and the reduction of CXCL5 expression in that cell line can decrease mitomycin-C resistance [37]. Similarly, CXCL5

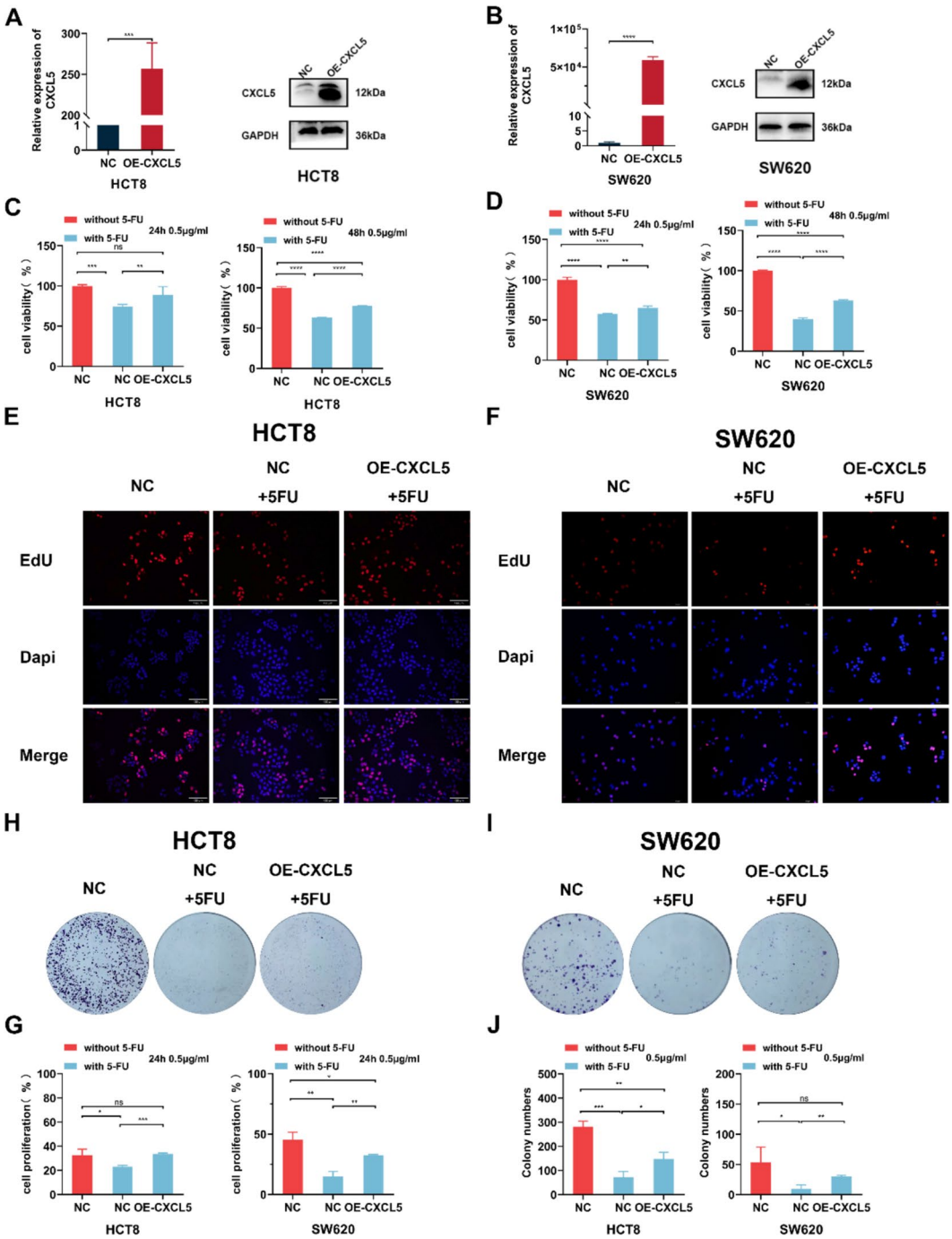

Fig. 4 Overexpression of CXCL5 promotes the resistance of CRC cells to 5-FU. **A** and **B** RT-qPCR and western blot assays confirmed the expression of CXCL5 in SW620 and HCT8 cells after transfection with a CXCL5 overexpression vector. ***$P<0.001$, ****$P<0.0001$. **C** and **D** CCK-8 assays indicated that higher CXCL5 levels enhanced the 5-FU resistance of CRC cells. **$P<0.01$, ***$P<0.001$, ****$P<0.0001$, *NS* not significant. **E–G** EdU assays revealed that higher CXCL5 levels increased the 5-FU resistance of CRC cells. Scale bar: 200 μm. *$P<0.05$, **$P<0.01$, ***$P<0.001$. *NS* not significant. **H–J** Colony formation assays demonstrated that upregulation of *CXCL5* strengthened the colony formation ability of SW620 and HCT8 cells. *$P<0.05$, **$P<0.01$, ***$P<0.001$, *NS* not significant

expression is significantly upregulated in sunitinib-resistant cells [38]. Evidence that the expression level of CXCL5 is connected with tumor malignancy and metastasis is mounting [39–41]. Thus, CXCL5 is potentially a novel target for tumor therapy [42–44].

CXCL5, a CXC-type chemokine with an ELR motif, is secreted by various immune cells and primarily acts as a

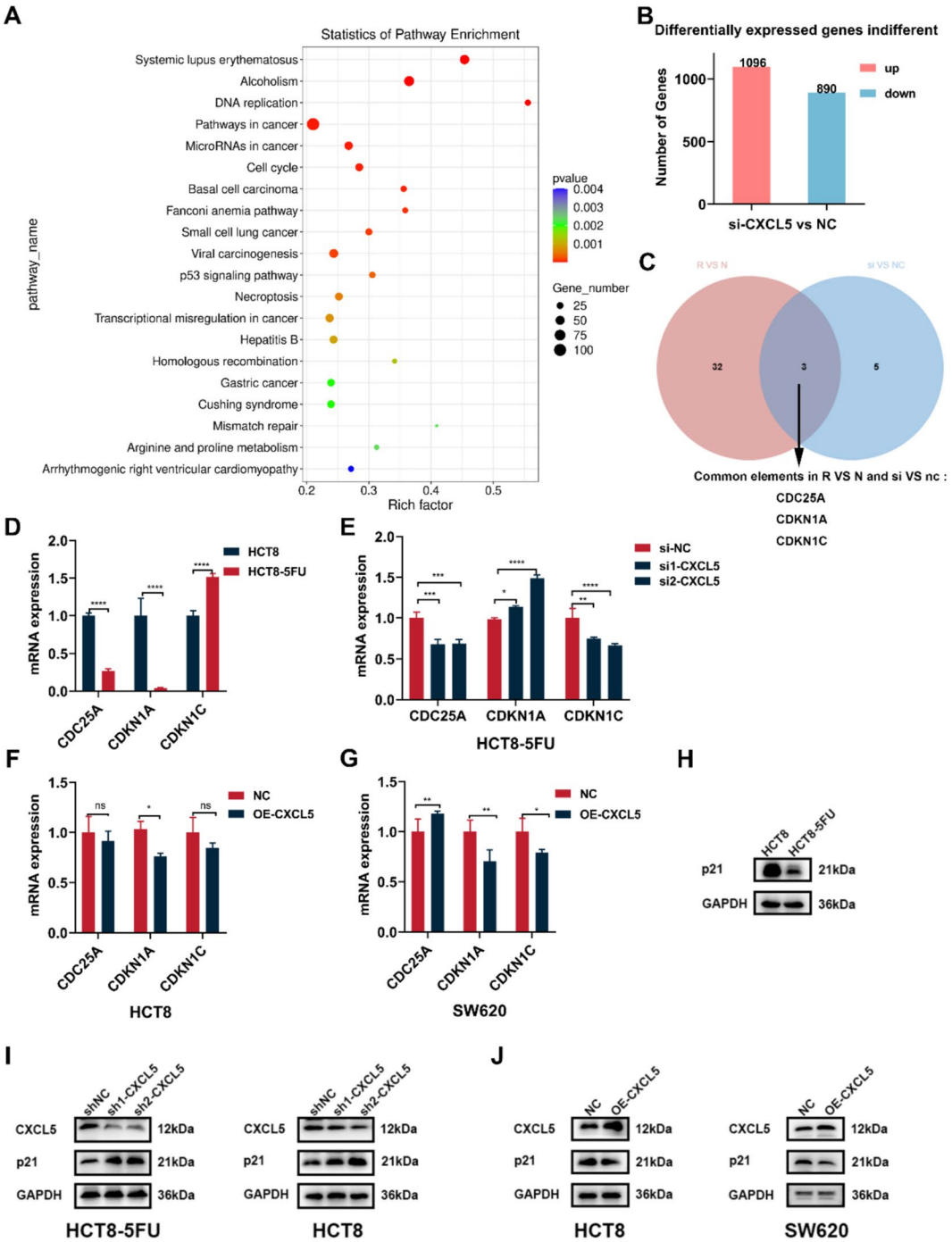

Fig. 5 Cell cycle suppressor gene *CDKN1A* (p21) is downregulated by CXCL5. **A** KEGG analysis of sequencing results of 5-FU-resistant cells showed differentially expressed genes enriched in cell cycle pathways. **B** RNA-seq revealed differentially expressed genes in HCT8-5FU cells in which *CXCL5* was downregulated. **C** Intersection of differentially expressed genes enriched in cell cycle pathways upon KEGG analysis of the two RNA-seq results. **D** RT-qPCR assays of cell cycle pathway-related genes in HCT8 and HCT8-5FU cells. $^{****}P<0.0001$. **E** RT-qPCR assays of cell cycle pathway-related genes in HCT8-5FU cells with downregulation of *CXCL5*. $^{*}P<0.05$, $^{**}P<0.01$, $^{***}P<0.001$, $^{****}P<0.0001$, *NS* not significant. **F** and **G** RT-qPCR assays were used to detect the effect of overexpression of *CXCL5* in HCT8 and SW620 cells on cell cycle pathway-related genes. $^{*}P<0.05$, $^{**}P<0.01$, *NS* not significant. **H** Western blot assays revealed that protein levels of p21 was lower in HCT8-5FU cells than that in HCT8 cells. **I** Western blot assays revealed the increased expression of p21 in HCT8-5FU and HCT8 cells which were transfected with shRNAs. **J** Western blot assays revealed the decreased expression of p21 in HCT8 and SW620 cells which were transfected with CXCL5 vectors. See also Figure S3

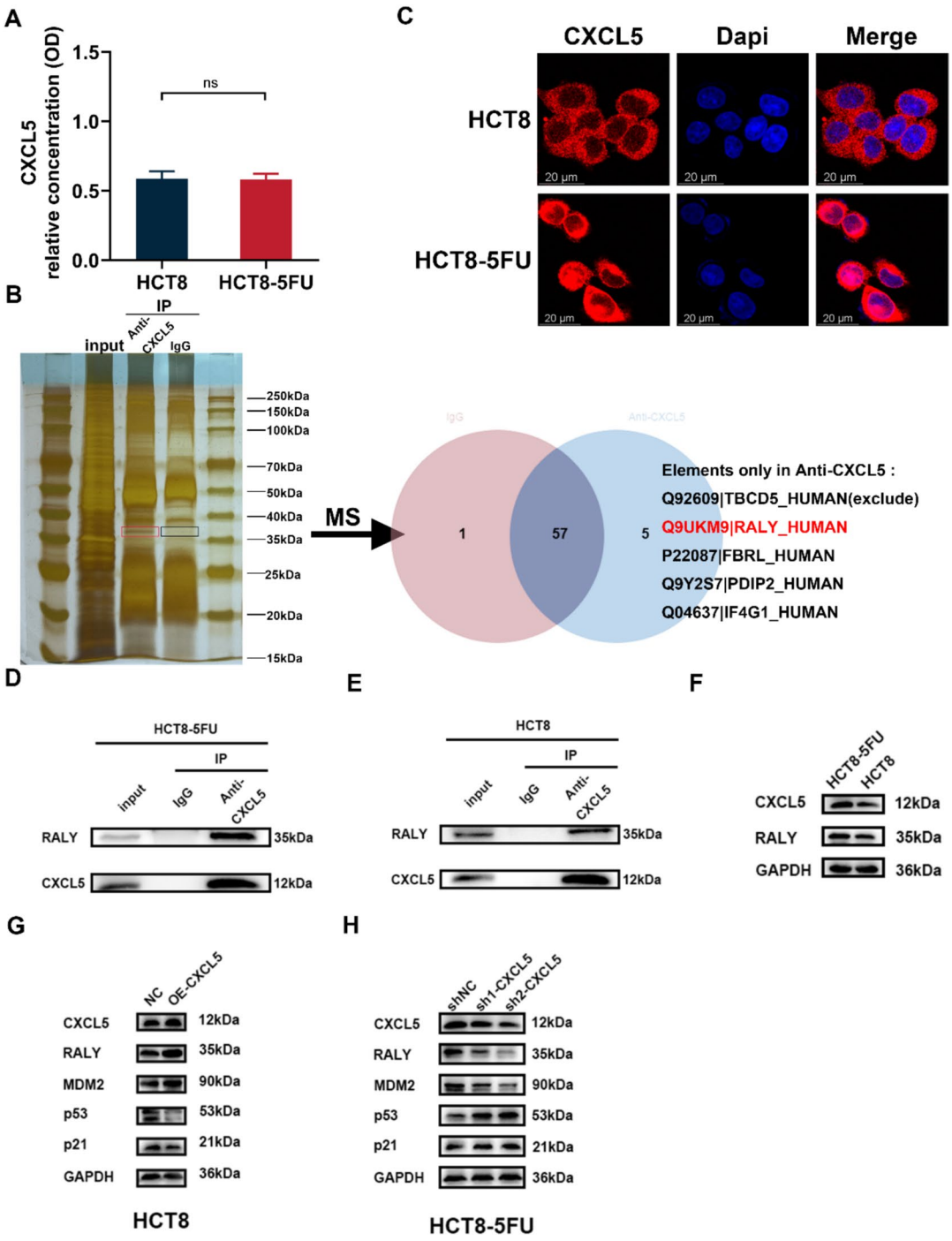

Fig. 6 CXCL5 modulates MDM2/p53 axis to inhibit p21 by binding to RALY. **A** ELISA assays showed that the secretion of CXCL5 did not differ between HCT8 and HCT8-5FU cells. *NS* not significant. **B** Silver staining and mass spectrometry assays revealed the identity of the specific binding protein of CXCL5. **C** Immunofluorescence showed that CXCL5 was expressed in the nuclei of HCT8-5FU cells. **D** and **E** Co-immunoprecipitation confirmed the specific binding of CXCL5 to RALY in HCT8-5FU and HCT8 cells. **F** Western blotting revealed that the expression of RALY was higher in HCT8-5FU cells than that in HCT8 cells. **G** and **H** Western blotting verified the effects of overexpression and downregulation of CXCL5 on the expression of RALY, MDM2, p53 and p21. See also Figure S4

ligand for CXCR2 [45]. CXCL5 contributes significantly to angiogenesis through the activation of CXCR2 [12]. CXCL5 recruits T/B lymphocytes, neutrophils, eosinophils, and other immune cells to specific regions during the immune response, contributing to anti-infection and antiviral activities [13]. It also enhances the adhesion and remodeling of

connective tissues [14]. Studies focused on CXCL5 and tumor progression have indicated that the CXCL5/CXCR2 axis drives tumor growth, stimulates angiogenesis, and aids in the invasion and activation of host cells [46, 47]. CXCL5 is regarded as an effective angiogenic factor with chemotactic effects on the vascular endothelium. It induces abundant angiogenesis during tumor progression through the actions of multiple signaling pathways. The possibility of targeted interventions against the molecular targets that initiate and promote vascular mimicry has also been explored. The inhibition of such key molecules can reduce the occurrence of vascular mimicry, thereby enhancing the effectiveness of tumor treatments. Although current research is still in the experimental stage, as a novel mode of tumor blood supply, vascular mimicry may be a new therapeutic target for tumor treatment in the future [48].

Here, we explored the novel role of CXCL5 in 5-FU resistance in CRC. We discovered that CXCL5 expression was upregulated in CRC 5-FU-resistant cells. At the beginning of this study, we attempted to find an association between the 5-FU concentration and CXCL5 expression, no such link was observed. Additional experiments demonstrated that CXCL5 boosts CRC cell proliferation and functions as a p53 pathway suppressor by binding to RALY in the nucleus. This is the first study in which the expression, function, and mechanism of action of CXCL5 in CRC resistance to 5-FU has been explored. Our results suggest that CXCL5 upregulation is associated with an increased tumor size and a poor prognosis. Gain- and loss-of-function experiments demonstrated that CXCL5 promotes CRC growth and increases the resistance to 5-FU treatment. One limitation of our study is that we were unable to explain the specific interaction between CXCL5 and RALY. Our work was focused on how CXCL5 affects drug resistance. In the future, additional problems related to drug resistance can be addressed via the use of other techniques, such as the screening potential drug resistance targets via CRISPR [49]. Moreover, we did not explore whether CXCL5 has the same cancer-promoting effects during the course of resistance to other forms of chemotherapy [50]. Much work remains to be done regarding the function and mechanisms of CXCL5 in tumor progression. Further studies should be conducted on the structure of the CXCL5–RALY interaction and other aspects. The interaction between CXCL5, RALY, and MDM2 will be carried out systematically in our future work. Our results also should be verified in patient-derived xenograft models [51–53].

Although CXCL5 is commonly identified as a ligand of CXCR2 in cancer tissues, it also interacts with other proteins to significantly contribute to tumorigenesis and cancer progression. According to the MS results of this study, CXCL5 in HCT8-5FU cells is mostly bound to nuclear proteins. As our experiments revealed the nuclear expression of CXCL5, we focused on the intranuclear function of CXCL5 in conferring 5-FU resistance in CRC. We verified that CXCL5 may inhibit p53 pathways by binding to RALY and subsequently downregulating p21 expression. Thus, CXCL5 is a potential target to enhance CRC cell sensitivity to 5-FU therapy.

Conclusion

In summary, our study revealed the high expression level of CXCL5 that promotes the 5-FU resistance of CRC cells and drives CRC development. CXCL5 can bind to RALY to promote the stability of MDM2, which suppresses the expression of p53/p21 (Fig. 6). Thus, CXCL5 may enhance the 5-FU resistance of CRC cells by promoting cell cycle progression. These results offer a fresh understanding of the involvement of CXCL5 in CRC and suggest that it may be a therapeutic target for CRC treatment.

Supplementary Information The online version contains supplementary material available at https://doi.org/10.1007/s12032-025-02801-6.

Acknowledgements Not applicable.

Author contributions WJX, XML, DSP designed the study. WJX wrote the manuscript. WJX, JJW, WCH performed the experiments. JMS and XMY collected samples and interpreted part of data. The manuscript was reviewed by all authors.

Funding This research was funded by the Medical Research Project of Jiangsu Provincial Health Commission (M2024038), the Social Development Projects of Key R&D Programs in Xuzhou (Grant KC23247), the Suqian Sci&Tech Program (Grant KY202304), and the Suqian Talent Xiongying Plan Project (Grant SQXY202436).

Data availability The raw RNA-seq data have been submitted to the NCBI Sequence Read Archive (SRA) database with the accession code PRJNA1189255 and PRJNA1190160.

Declarations

Competing interests The authors declare no competing interests.

Ethical approval The research was approved by the Ethics Committee of Xuzhou Medical University (Xuzhou, China).

Consent to participate Consent forms were signed by all patients. This study adhered to the National Institutes of Health's Guide for the Care and Use of Laboratory Animals. The Committee on the Ethics of Animal Experiments at Xuzhou Medical University approved the protocol.

Consent for publication Patients gave written informed consent for the research use of their clinical materials.

References

1. Bray F, Laversanne M, Sung H, et al. Global cancer statistics 2022: GLOBOCAN estimates of incidence and mortality

worldwide for 36 cancers in 185 countries. CA Cancer J Clin. 2024;74(3):229–63. https://doi.org/10.3322/caac.21834.
2. Siegel RL, Giaquinto AN, Jemal A. Cancer statistics, 2024. CA Cancer J Clin. 2024;74(1):12–49. https://doi.org/10.3322/caac.21820.
3. Sonkin D, Thomas A, Teicher BA. Cancer treatments: Past, present, and future. Cancer Genet. 2024;286–287:18–24. https://doi.org/10.1016/j.cancergen.2024.06.002.
4. Zlotnik A, Yoshie O. The chemokine superfamily revisited. Immunity. 2012;36(5):705–16. https://doi.org/10.1016/j.immuni.2012.05.008.
5. Colotta F, Allavena P, Sica A, Garlanda C, Mantovani A. Cancer-related inflammation, the seventh hallmark of cancer: links to genetic instability. Carcinogenesis. 2009;30(7):1073–81. https://doi.org/10.1093/carcin/bgp127.
6. Korbecki J, Bosiacki M, Barczak K, et al. Involvement in tumorigenesis and clinical significance of CXCL1 in reproductive cancers: breast cancer, cervical cancer, endometrial cancer, ovarian cancer and prostate cancer. Int J Mol Sci. 2023;24(8):7262. https://doi.org/10.3390/ijms24087262.
7. Zhang H, Ye YL, Li MX, et al. CXCL2/MIF-CXCR2 signaling promotes the recruitment of myeloid-derived suppressor cells and is correlated with prognosis in bladder cancer. Oncogene. 2017;36(15):2095–104. https://doi.org/10.1038/onc.2016.367.
8. Liu Y, Xiao J, Cai J, et al. Single-cell immune profiling of mouse liver aging reveals Cxcl2+ macrophages recruit neutrophils to aggravate liver injury. Hepatology. 2024;79(3):589–605. https://doi.org/10.1097/HEP.0000000000000590.
9. Qi YL, Li Y, Man XX, et al. CXCL3 overexpression promotes the tumorigenic potential of uterine cervical cancer cells via the MAPK/ERK pathway. J Cell Physiol. 2020;235(5):4756–65. https://doi.org/10.1002/jcp.29353.
10. Liu Q, Li A, Tian Y, et al. The CXCL8-CXCR1/2 pathways in cancer. Cytokine Growth Factor Rev. 2016;31:61–71. https://doi.org/10.1016/j.cytogfr.2016.08.002.
11. Walz A, Strieter RM, Schnyder S. Neutrophil-activating peptide ENA-78. Adv Exp Med Biol. 1993;351:129–37. https://doi.org/10.1007/978-1-4615-2952-1_14.
12. Zhang W, Wang H, Sun M, et al. CXCL5/CXCR2 axis in tumor microenvironment as potential diagnostic biomarker and therapeutic target. Cancer Commun (Lond). 2020;40(2–3):69–80. https://doi.org/10.1002/cac2.12010.
13. Griffith JW, Sokol CL, Luster AD. Chemokines and chemokine receptors: positioning cells for host defense and immunity. Annu Rev Immunol. 2014;32:659–702. https://doi.org/10.1146/annurev-immunol-032713-120145.
14. Duchene J, Lecomte F, Ahmed S, et al. A novel inflammatory pathway involved in leukocyte recruitment: role for the kinin B1 receptor and the chemokine CXCL5. J Immunol. 2007;179(7):4849–56.
15. Park JY, Park KH, Bang S, et al. CXCL5 overexpression is associated with late stage gastric cancer. J Cancer Res Clin Oncol. 2007;133(11):835–40. https://doi.org/10.1007/s00432-007-0225-x.
16. Begley LA, Kasina S, Mehra R, et al. CXCL5 promotes prostate cancer progression. Neoplasia. 2008;10(3):244–54. https://doi.org/10.1593/neo.07976.
17. Mollaoglu G, Jones A, Wait SJ, et al. The lineage-defining transcription factors SOX2 and NKX2-1 determine lung cancer cell fate and shape the tumor immune microenvironment. Immunity. 2018;49(4):764-779.e9. https://doi.org/10.1016/j.immuni.2018.09.020.
18. Sakabe T, Azumi J, Umekita Y, et al. Expression of cancer stem cell-associated DKK1 mRNA serves as prognostic marker for hepatocellular carcinoma. Anticancer Res. 2017;37(9):4881–8. https://doi.org/10.21873/anticanres.11897.
19. Li A, King J, Moro A, et al. Overexpression of CXCL5 is associated with poor survival in patients with pancreatic cancer. Am J Pathol. 2011;178(3):1340–9. https://doi.org/10.1016/j.ajpath.2010.11.058.
20. Rubie C, Frick VO, Wagner M, et al. ELR+ CXC chemokine expression in benign and malignant colorectal conditions. BMC Cancer. 2008;8:178. https://doi.org/10.1186/1471-2407-8-178.
21. Hu H, Zhao K, Fang D, et al. The RNA binding protein RALY suppresses p53 activity and promotes lung tumorigenesis. Cell Rep. 2023;42(4): 112288. https://doi.org/10.1016/j.celrep.2023.112288.
22. Mao P, Wang T, Du CW, Yu X, Wang MD. CXCL5 promotes tumorigenesis and angiogenesis of glioblastoma via JAK-STAT/NF-κb signaling pathways. Mol Biol Rep. 2023;50(10):8015–23. https://doi.org/10.1007/s11033-023-08671-3.
23. Bièche I, Chavey C, Andrieu C, et al. CXC chemokines located in the 4q21 region are up-regulated in breast cancer. Endocr Relat Cancer. 2007;14(4):1039–52. https://doi.org/10.1677/erc.1.01301.
24. Mo M, Li Y, Hu X. Serum CXCL5 level is associated with tumor progression in penile cancer. Biosci Rep. 2021;41(1):BSR20202133. https://doi.org/10.1042/BSR20202133.
25. Soler-Cardona A, Forsthuber A, Lipp K, et al. CXCL5 facilitates melanoma cell-neutrophil interaction and lymph node metastasis. J Invest Dermatol. 2018;138(7):1627–35. https://doi.org/10.1016/j.jid.2018.01.035.
26. Bai L, Yao N, Qiao G, Wu L, Ma X. CXCL5 contributes to the tumorigenicity of cervical cancer and is post-transcriptionally regulated by miR-577. Int J Clin Exp Pathol. 2020;13(12):2984–93.
27. Gao Y, Guan Z, Chen J, et al. CXCL5/CXCR2 axis promotes bladder cancer cell migration and invasion by activating PI3K/AKT-induced upregulation of MMP2/MMP9. Int J Oncol. 2015;47(2):690–700. https://doi.org/10.3892/ijo.2015.3041.
28. Liu Y, Qu HC, Huang Y. Renal clear cell carcinoma-derived CXCL5 drives tumor-associated fibroblast formation and facilitates cancer progression. Pathol Res Pract. 2023;244: 154319. https://doi.org/10.1016/j.prp.2023.154319.
29. Dang H, Wu W, Wang B, et al. CXCL5 plays a promoting role in osteosarcoma cell migration and invasion in autocrine- and paracrine-dependent manners. Oncol Res. 2017;25(2):177–86. https://doi.org/10.3727/096504016X14732772150343.
30. Chen G, Teng Z, Zhu Z, Li X. miR-145-3p hampers the malignant progression of esophageal carcinoma via CXCL5 downregulation. Anal Cell Pathol (Amst). 2022;2022:5418356. https://doi.org/10.1155/2022/5418356.
31. Qiu WZ, Zhang HB, Xia WX, et al. The CXCL5/CXCR2 axis contributes to the epithelial-mesenchymal transition of nasopharyngeal carcinoma cells by activating ERK/GSK-3β/snail signalling. J Exp Clin Cancer Res. 2018;37(1):85. https://doi.org/10.1186/s13046-018-0722-6.
32. Chang W, Chang Q, Lu H, Liu S, Li Y, Chen C. MicroRNA-873-5p suppresses cell malignant behaviors of thyroid cancer via targeting CXCL5 and regulating P53 pathway. Hum Vaccin Immunother. 2022;18(5):2065837. https://doi.org/10.1080/21645515.2022.2065837.
33. Miyazaki H, Patel V, Wang H, Ensley JF, Gutkind JS, Yeudall WA. Growth factor-sensitive molecular targets identified in primary and metastatic head and neck squamous cell carcinoma using microarray analysis. Oral Oncol. 2006;42(3):240–56. https://doi.org/10.1016/j.oraloncology.2005.07.006.
34. Lee SJ, Kim JE, Kim ST, et al. The correlation between serum chemokines and clinical outcome in patients with advanced biliary tract cancer. Transl Oncol. 2018;11(2):353–7. https://doi.org/10.1016/j.tranon.2018.01.007.
35. Zhang D, Zhou J, Tang D, et al. Neutrophil infiltration mediated by CXCL5 accumulation in the laryngeal squamous cell carcinoma

microenvironment: A mechanism by which tumour cells escape immune surveillance. Clin Immunol. 2017;175:34–40. https://doi.org/10.1016/j.clim.2016.11.009.
36. Lee NH, Ma Y, Ang CS, et al. CXCL5 knockdown attenuated gemcitabine resistance of pancreatic cancer through regulation of cancer cells and tumour stroma. Am J Transl Res. 2023;15(4):2676–89.
37. Wang C, Li A, Yang S, Qiao R, Zhu X, Zhang J. CXCL5 promotes mitomycin C resistance in non-muscle invasive bladder cancer by activating EMT and NF-κB pathway. Biochem Biophys Res Commun. 2018;498(4):862–8. https://doi.org/10.1016/j.bbrc.2018.03.071.
38. Giuliano S, Dufies M, Ndiaye PD, et al. Resistance to lysosomotropic drugs used to treat kidney and breast cancers involves autophagy and inflammation and converges in inducing CXCL5. Theranostics. 2019;9(4):1181–99. https://doi.org/10.7150/thno.29093.
39. Zhao J, Ou B, Han D, et al. Tumor-derived CXCL5 promotes human colorectal cancer metastasis through activation of the ERK/Elk-1/Snail and AKT/GSK3β/β-catenin pathways. Mol Cancer. 2017;16:70. https://doi.org/10.1186/s12943-017-0629-4.
40. Mao Z, Zhang J, Shi Y, et al. CXCL5 promotes gastric cancer metastasis by inducing epithelial-mesenchymal transition and activating neutrophils. Oncogenesis. 2020;9(7):63. https://doi.org/10.1038/s41389-020-00249-z.
41. Li X, Wang M, Gong T, et al. A S100A14-CCL2/CXCL5 signaling axis drives breast cancer metastasis. Theranostics. 2020;10(13):5687–703. https://doi.org/10.7150/thno.42087.
42. Jia X, Wei S, Xiong W. CXCL5/NF-κB pathway as a therapeutic target in hepatocellular carcinoma treatment. J Oncol. 2021;2021:9919494. https://doi.org/10.1155/2021/9919494.
43. Kawamura M, Toiyama Y, Tanaka K, et al. CXCL5, a promoter of cell proliferation, migration and invasion, is a novel serum prognostic marker in patients with colorectal cancer. Eur J Cancer. 2012;48(14):2244–51. https://doi.org/10.1016/j.ejca.2011.11.032.
44. Luo M, Hu Z, Kong Y, Li L. MicroRNA-432-5p inhibits cell migration and invasion by targeting CXCL5 in colorectal cancer. Exp Ther Med. 2021;21(4):301. https://doi.org/10.3892/etm.2021.9732.
45. Deng J, Jiang R, Meng E, Wu H. CXCL5: A coachman to drive cancer progression. Front Oncol. 2022;12: 944494. https://doi.org/10.3389/fonc.2022.944494.
46. Chen C, Xu ZQ, Zong YP, et al. CXCL5 induces tumor angiogenesis via enhancing the expression of FOXD1 mediated by the AKT/NF-κB pathway in colorectal cancer. Cell Death Dis. 2019;10(3):178. https://doi.org/10.1038/s41419-019-1431-6.
47. Huang Z, Zhang M, Chen G, et al. Bladder cancer cells interact with vascular endothelial cells triggering EGFR signals to promote tumor progression. Int J Oncol. 2019;54(5):1555–66. https://doi.org/10.3892/ijo.2019.4729.
48. Dang SM, Yang D, Wang ZY, et al. Vasculogenic mimicry: A pivotal mechanism contributing to... : Oncology and Translational Medicine. Accessed May 3, 2025. https://journals.lww.com/otm/fulltext/2024/06000/vasculogenic_mimicry__a_pivotal_mechanism.4.aspx
49. Liu H, Wang P. CRISPR screening and cell line IC50 data reveal novel key genes for trametinib resistance. Clin Exp Med. 2024;25(1):21. https://doi.org/10.1007/s10238-024-01538-2.
50. He S, Xiao X, Lei R, et al. Establishment of breast phyllodes tumor cell lines preserving the features of phyllodes tumors. BIO Integration. 2023;4(1):7–17. https://doi.org/10.15212/bioi-2022-0025.
51. Li R, Huang Y, Liu H, Dilger JP, Lin J. Abstract 2162: Comparing volatile and intravenous anesthetics in a mouse model of breast cancer metastasis. Can Res. 2018;78(13_Supplement):2162. https://doi.org/10.1158/1538-7445.AM2018-2162.
52. Kang ZR, Jiang S, Han JX, et al. Deficiency of BCAT2-mediated branched-chain amino acid catabolism promotes colorectal cancer development. Biochimica et Biophysica Acta (BBA)—Molecular Basis of Disease. 2024;1870(2): 166941. https://doi.org/10.1016/j.bbadis.2023.166941.
53. Lee SJ, Jeon SH, Cho S, et al. hsa-miR-CHA2, a novel microRNA, exhibits anticancer effects by suppressing cyclin E1 in human non-small cell lung cancer cells. Biochimica et Biophysica Acta (BBA)—Molecular Basis of Disease. 2024;1870(6): 167250. https://doi.org/10.1016/j.bbadis.2024.167250.